Replacement Effects of Neutral Amino Acid Residues of Different Molecular Volumes in the Retinal Binding Cavity of Bacteriorhodopsin on the Dynamics of Its Primary Process

Stephan L. Logunov,* Mostafa A. El-Sayed,* and Janos K. Lanyi‡
*School of Chemistry and Biochemistry, Georgia Institute of Technology, Atlanta, Georgia 30332-0400, and ‡Department of Biophysics and Physiology, University of Irvine, Irvine, California 92717 USA

ABSTRACT We have determined the rate and quantum yield of retinal photoisomerization, the spectra of the primary transients, and the energy stored in the K intermediate in the photocycle of some bacteriorhodopsin mutants (V49A, A53G, and W182F) in which residue replacements are found to change the Schiff base deprotonation kinetics (and thus the protein-retinal interaction). Because of their change in the local volume resulting from these individual replacements, these substitutions perturb the proton donor-acceptor relative orientation change and thus the Schiff base deprotonation kinetics. These replacements are thus expected to change the charge distribution around the retinal, which controls its photoisomerization dynamics. Subpicosecond transient spectroscopy as well as photoacoustic technique are used to determine the retinal photoisomerization rate, quantum yield, and the energy stored in the K-intermediate for these mutants. The results are compared with those obtained for wild-type bacteriorhodopsin and other mutants in which charged residues in the cavity are replaced by neutral ones. In some of the mutants the rate of photoisomerization is changed, but in none is the quantum yield or the energy stored in the K intermediate altered from that in the wild type. These results are discussed in terms of the shapes of the potential energy surfaces of the excited and ground states of retinal in the perpendicular configuration within the protein and the stabilization of the positive charge in the ground and the excited state of the electronic system of retinal.

INTRODUCTION

Bacteriorhodopsin (bR) functions as a light-driven proton pump and converts light into chemical energy by pumping protons across the bacterial membrane. Upon absorption of light, bacteriorhodopsin undergoes a photocycle that involves spectroscopically distinctive intermediates (Oesterhelt et al., 1974; Braiman et al., 1988; Lanyi, 1993). The protein contains an all-*trans* retinal chromophore, which isomerizes to 13-*cis* within 500 fs after the absorption of a photon. The ground state of light-adapted bR absorbs at 568 nm and has an extinction coefficient of 63,000 M^{-1} cm^{-1}. The first intermediate, which could be trapped at low temperature, is the K intermediate, with a spectral maximum at λ = 595 nm and an extinction coefficient of 55,000 M^{-1} cm^{-1}. This spectrum strongly overlaps with the bR ground state. Electron diffraction analysis of bR structure gives information about the spatial arrangement of amino acids around the retinal chromophore (Henderson et al., 1990).

Site-directed mutagenesis provides an effective method of studying the important questions regarding protein structure and function. It has been shown previously that perturbation of charged amino acid residues of protein in the vicinity of the Schiff base of retinal affect the rate of photoisomerization (Song et al., 1993; Logunov et al., 1996). In the mutants D85N, R82Q, and D212N, in which the charged residues of amino acids in the vicinity of the Schiff base of retinal were changed to neutral ones, the rate of photoisomerization was slowed down by up to 20-fold (Song et al., 1993). The results suggest that the distribution of the charged groups around the retinal Schiff base controls the rate of the isomerization. If this is correct, it means that modification of the geometry of the proton donor and acceptor (the Schiff base D85) charged pair, mediated by bound water (Brown et al., 1995), may also affect the rate of photoisomerization dynamics and the photocycle. It has to be noted that replacement of any of the amino acids that form the retinal pocket would change the geometry of the retinal-protein interaction (Brown et al., 1995), so it may also change the rate of the photoisomerization and its quantum yield. To answer this question we have studied the dynamics of photoisomerization in mutants in which the neutral amino acids Val-49, Ala-53, or Trp-182 residues in the retinal-binding pocket are replaced by Ala, Gly, or Phe, respectively. These amino acids and others are proposed to constitute the retinal binding pocket (Wu et al., 1992). It was proposed (Brown et al., 1995) that in V49A and A53G mutants the geometrical arrangement of the Schiff base and Asp85 is changed. In the W182F mutant it was proposed (Yamazaki et al., 1995) that Trp182 interacts with the retinal side chain through the 9-methyl group. All of these residue replacements are known to change the rate of proton transfer from the Schiff base to Asp85 in the photocycle.

MATERIALS AND METHODS

Bacteriorhodopsin-containing cells were grown from the master slants of *Halobacterium halobium* ET1-001 strain, kindly provided to us by Professor Bogomolni at UC Santa Cruz. The purple membranes from this strain

Received for publication 8 June 1995 and in final form 19 March 1996.

Address reprint requests to Dr. Moustafa A. El-Sayed, Department of Chemistry and Biochemistry, Georgia Institute of Technology, Atlanta, GA 30332. Tel.: 404-894-0292; Fax: 404-894-0294; E-mail: mostafa.el-sayed@chemistry.gatech.edu.

0006-3495/96/06/2875/07 $2.00

and the mutants V49A, A53G, and W182F were isolated and purified as described previously (Oesterhelt and Stoeckenius, 1974). All measurements were completed at room temperature in aqueous solution. The pH was adjusted by adding 100 mM phosphate buffer. The final salt concentration did not exceed 30 mM and was not expected to affect the acoustic properties of water. All samples were light adapted.

The laser system, transient absorption, and photoacoustic spectroscopic measurements were described previously (Logunov et al., 1994, 1996). Transient absorption data were collected on a multichannel, charge-coupled device, nitrogen-cooled (EV-1024; Princeton Instruments) detector for direct spectral measurements. For decay measurements at a single wavelength, a couple of photodiodes are used.

The analysis of the photoacoustic signals was analogous to that described previously (Braslavsky and Heihoff, 1989; Rohr et al., 1992a). A solution of $CoCl_2$ has been used as a calorimetric reference. The sample suspension was stirred after every 100 shots. The optical density of all samples was adjusted to 0.4 at the excitation wavelength.

The amount of heat measured in the photoacoustic measurements was

$$Q = C\alpha E_{exc}(1-10^{-A}), \quad (1)$$

where E_{exc} is the laser energy; A is the absorbance of the sample; C is the proportionality constant that depends on the geometrical factor, solvent parameters, and thermoelastic properties of the media; and α is the fraction of the absorbed energy that dissipate into the solvent. The fraction of the absorbed energy stored in the bR system is $(1 - \alpha)$. $(1 - \alpha)$ is equal to $\Phi E_i/E_{exc}$, where Φ is the isomerization quantum yield, E_i is the energy stored in the intermediate formed on the time scale of the photoacoustic experiment, and E_{exc} is the excitation energy. Because this is equal to 100 ns, E_i is then the energy stored in K_{590} (which decays in 1.5 μs).

In principle, the transient absorption experiment should enable one to determine the quantum yield of photoisomerization to the K intermediate if its absorption is separated from the bleached parent absorption and if their molar extinction coefficients are known. Unfortunately, this is not the situation; the two spectra overlap for the bR variants studied here. To deconvolute them, a lower limit of the quantum yield is needed. This can be obtained from the photoacoustic measurements (as shown below) if one assumes an upper limit for the energy stored in the K intermediate to be equal to the energy of the 0–0 band of the parent. The quantum yield of photoisomerization is determined by the following method. This is done from the transient absorption data with use of the lower limit of quantum yield from photoacoustic data. The total amount of the excited bR molecules could be obtained from the amplitude of the bleaching signal at zero time after excitation by the subpicosecond laser pulse. At zero time, only bleaching of the ground state and the absorption of the excited state could be observed. At a delay time of a few tens of picoseconds, only the absorption of the K-intermediate and bleached ground state are observed. To the latter spectrum we added different spectra with the shape of the ground state spectrum of bR, but each was multiplied by different fractional constants until a reasonable spectrum for the K intermediate was obtained. The initial value for this fractional factor was taken to be equal the lower limit of quantum yield value obtained from the photoacoustic data. The absorption spectrum of the K intermediate so obtained was compared with the nanosecond transient absorption data when available, to check on our fitting procedure. The fractional constant that gave the best spectrum is the quantum yield of photoisomerization. This will be an average quantum yield for the different isomers present in the ground state of the bR variants being studied. Once the photoisomerization quantum yield is determined, one can use the photoacoustic results to obtain the apparent (average) values for the energy stored in the K-type intermediate of these bR variants.

RESULTS AND DISCUSSION

Photoacoustic data

The time scale of this experiment is determined by the integration time of heat dissipation, which is determined by the pinhole size. For our measurements the time constant of the studied process is determined by the beam size in the cuvette (D), which is equal to 0.2 mm. Using the equation $\tau = D/v$, where v is the speed of sound in water, we obtained τ = 130 ns. The slopes of the plots of the photoacoustic signal versus laser power for the studied mutants and the reference ($CoCl_2$) with matched absorbance are shown in Fig. 1. The amount of heat and thus the amount of energy stored in the sample are extracted from these measurements.

It was shown previously (Rohr et al., 1992a) that for experiments with short laser pulses, when only the ground state of bR is excited, and the integration time is shorter than the lifetime of the K-intermediate, the energy balance equation may be reduced to (Rohr et al., 1992a; Logunov et al., 1996)

$$1 - \alpha \approx \Phi E_K/E_{exc}, \quad (2)$$

where α is the ratio of the slopes of the observed linear relationship between the photoacoustic signal and the laser power for bR solution to that for $CoCl_2$ solution. This gives the amount of the energy dissipated to the solvent in the bR solution. $(1 - \alpha)$ is the fraction of the energy stored in the sample, Φ is the quantum yield of photoisomerization, E_K is the energy of the K intermediate, E_{exc} is the excitation energy. The uncertainty in the calculation of the K-intermediate quantum yield and the energy content originates from the fact that volume changes also may contribute to the photoacoustic signal. This factor has been shown previously (Schulenberg et al., 1994) to be as large as 10–15% for monomerized bR, after excitation with a 10-ns laser pulse. However, when subpicosecond pulses are used, this effect is as small as 5% (Rohr et al., 1992b). We will not take this

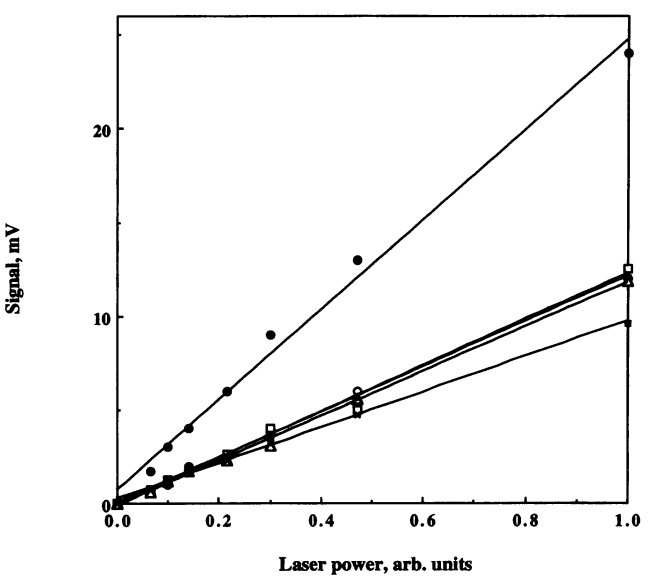

FIGURE 1 Plots of photoacoustic signal versus laser energy of mutants W182F (□), V49A (△), A53G (*), wild-type bR (○), and the reference sample $CoCl_2$ (●). The ratio of the slopes corresponds to the amount of the heat produced in the sample.

effect into consideration, because the accuracy of our measurements will be determined by the larger errors involved in determining the amplitude of the transient signal for the K and other overlapping intermediates. Because of the strong overlap of the absorption of these mutants with their intermediates and because of the weak transient signal, the errors in Q and E_K would be higher than for wild-type bR, which has less absorption overlapping with its intermediates (Logunov et al., 1996). This introduces error in the Φ measurements (due to the deconvolution procedure) that can be 10–15%.

From these data one can estimate the quantum yield of the retinal photoisomerization process, assuming that the upper limit value for the energy of K to be that of the 0–0 transition of the ground-state absorption. Alternatively, the lower limit for the energy content in the K-intermediate could be obtained, assuming that the quantum yield of isomerization is unity. The results obtained based on the photoacoustic data and these assumptions are shown in Table 1.

Transient absorption

The rate of photoisomerization for native bR was measured previously and is found to be 500 fs (Petrich et al., 1987; Mathies et al., 1988). The quantum yield of isomerization was found to be about 0.6, in agreement with previous studies (Goldschmidt et al., 1977; Tittor and Oesterhelt, 1990; Xie, 1990; Rohr et al., 1992a; Logunov et al., 1994).

The kinetics of the photocycle in V49A, W182F, and A53G are different from that in wild bR. The rate of the Schiff base deprotonation becomes significantly smaller in comparison with that in wild-type bR (Table 2) by replacement of Trp-182 with phenylalanine (Yamazaki et al., 1995). This may change the interaction of Trp-182 with the 9-methyl group of retinal. On the basis of low-temperature ultraviolet/visible and Fourier transform infrared difference spectroscopy (Yamazaki et al., 1995), Trp-182 interacts strongly with the retinal, and may form part of the retinal binding pocket. This residue could directly or indirectly influence the configuration of retinal.

The basic features of the photoisomerization of W182F (the decay of both the ground-state bleach and the excited-state absorption, as well as the absorption rise time of the J- and K-like intermediates) after excitation with a 500-fs laser pulse are similar to those in the native bR. The subpicosecond dynamics of the native bR was measured in this apparatus previously (Song et al., 1993; Logunov et al., 1994), and the lifetime of excited state was found to be 500 ± 100 fs. The maximum of the retinal excited state of W182F is located at 470 nm (Fig. 2). The excited state of W182F decays with a lifetime of 800 ± 100 fs (*inset* at the top of Fig. 2). This is longer than in wild-type bR. There is also a slow component in the decay of the excited state with a lifetime longer than 20 ps. Unfortunately, the isomeric composition of W182F, V49A, and A53G is not known. The multiexponential decay of the excited state may be due to the presence of different isomers. The ground-state recovery has two components with lifetimes of 800 fs and 5 ps (*inset* at the bottom of Fig. 2). The fit parameters are shown in Table 3. The fast component is due to formation of the J-intermediate and recovery of the ground-state bR. The lifetime of this component is close to the lifetime of the excited-state decay, measured at 480 nm. The slower component reflects the formation of the K-state (Fig. 2, *inset* at the bottom). For quantum yield determination we used the procedure described in Materials and Methods. The quantum yield analysis gave the value of 0.65 ± 0.1. The shape of the K-spectrum from our analysis is shown in Fig. 3. The maximum for the K-intermediate was found to be located at 595 nm (wild-type bR), 600 nm (W182F), 595 nm (A53G), and 595 nm (V49A).

The spectra of studied mutants are similar to native bR, for which the excited-state absorption maximum is at 480 nm and 475 nm for A53G and V49A, respectively. The maxima of the bleached ground states are at 566 nm and 563 nm for A53G and V49A, respectively (see Figs. 4 and 5). The lifetime of the excited state was found to be 500 ± 100 fs for A53G and 1.0 ± 0.08 ps for V49A (see the *insets* at the top of Figs. 4 and 5). All decay curves show biexponential behavior. The slow component has an amplitude of 0.18 and a lifetime of 5 ps for A53G, and 0.2 and 20 ps for V49A (Table 3). Previously (Logunov et al., 1996) we showed that the relative amplitudes of the fast and slow components in the kinetics of the excited-state decay of mutants D212N, D85N, R82Q and deionized blue bR correlate well with the ratio of all-*trans* to 13-*cis* isomer composition (Song et al., 1995). Thus, the relative amplitude of the slow component in the decay of the retinal in perturbed bR seems to monitor the percentage of the isomer that is different from the all-*trans* form. Based on this conclusion, the slow component in the decay of the excited state in the present mutants is assigned to the presence of isomers different from the all-*trans* isomer. The bleaching of the ground-state recovery has three components; the first one has a lifetime equal to the decay of the excited state. The second component has a slightly longer lifetime, reflecting the formation of the K-intermediate (*insets* at the bottom of Figs. 4 and 5). The third one is an offset due to the difference between the ground state and the K-intermediate absorption at this wavelength. The lifetimes of the

TABLE 1 Lower limits of quantum yield of isomerization and energy of the K-intermediate, obtained from photoacoustic measurements and Eq. 2

Sample	Φ_{lower}	E_K (kJ/mol)
Wild bR*	0.48	97.0
A53G	0.39	78.5
W182F	0.52	75.6
V49A	0.51	104.4

*Wild bR data were taken from (Logunov et al., 1996)

TABLE 2 The parameters of the M state formation and decay, and parameters of the primary processes

Sample	*M* rise, average lifetime (μs)	*M* decay, average lifetime (ms)	Primary processes*			
			Φ_{iso}	τ_{iso}[‖] (ps)	τ_K (ps)	E_K (kJ/mol)
Wild-type bR	77.2[#]	6.4[#]	0.6	0.5	3.0	170
D212N, pH 4.4	100.0[§]	12.0[¶]	0.65	3.0	5.0	180
D85N, pH 4.5	—	—	0.7	5.3	4.0	180
Blue bR	—	—	0.7	9.5	5.0	170
R82Q, pH 4.5	—	—	0.6	3.2	5.0	180
V49A	1000[¶]	10.0[¶]	0.6	1.0	4.0	160
A53G	33.0[¶]	5.0[¶]	0.6	0.5	3.0	170
W182F	700[¶]	612[¶]	0.65	0.8	5.0	170

Quantum yield of photoisomerization, lifetime of photoisomerization, lifetime of the K-intermediate rise, and the energy content in the K-intermediate for wild-type bR, mutants with charged amino acid residues substituted to the neutral ones (D85N, R82Q, D212N) and deionized blue bR (Logunov et al., 1996), and mutants studied in the present paper (A53G, V49A, and W182F).

*Data for D212N, D85N, R82Q, and blue bR were taken from Logunov et al. (1996).

[#]Brown et al., 1994.

[§]Needleman et al., 1991.

[¶]Brown et al., 1994; Yamazaki et al., 1995.

[‖]τ_{aver} for multiexponential processes was calculated as $\tau_{aver} = \Sigma A_i \tau_i$, where A_i is relative amplitude of the component with lifetime of τ_i. The slow component in the decay of the excited state for mutants V49A and W182F was not taken into account.

fast components are those for the decay of the excited state, whereas the lifetimes of the second components are found to be 4 and 7 ps for A53G and V49A, respectively. Analysis of the quantum yield of the photoisomerization gave the value of about 0.6 ± 0.1 for both mutants. The deconvoluted absorption spectra of the excited states and the those for the K-intermediate are shown in Fig. 3.

The values determined for the quantum yield of photoisomerization and the energy content of the K-intermediate are average numbers for the different isomers of retinal present in perturbed bR. In these samples, light-adapted bR does not contain 100% all-*trans* isomer. As was discussed above, the slow component, with an amplitude of 0.18–0.2 in the excited-state decay of mutants A53G, W182F, and V49A, is mostly likely due to isomers different from all-*trans* configuration. If we want to compare the dynamics of the retinal in mutants with that of wild-type bR, we must obtain these parameters for all-*trans* retinal. We can esti-

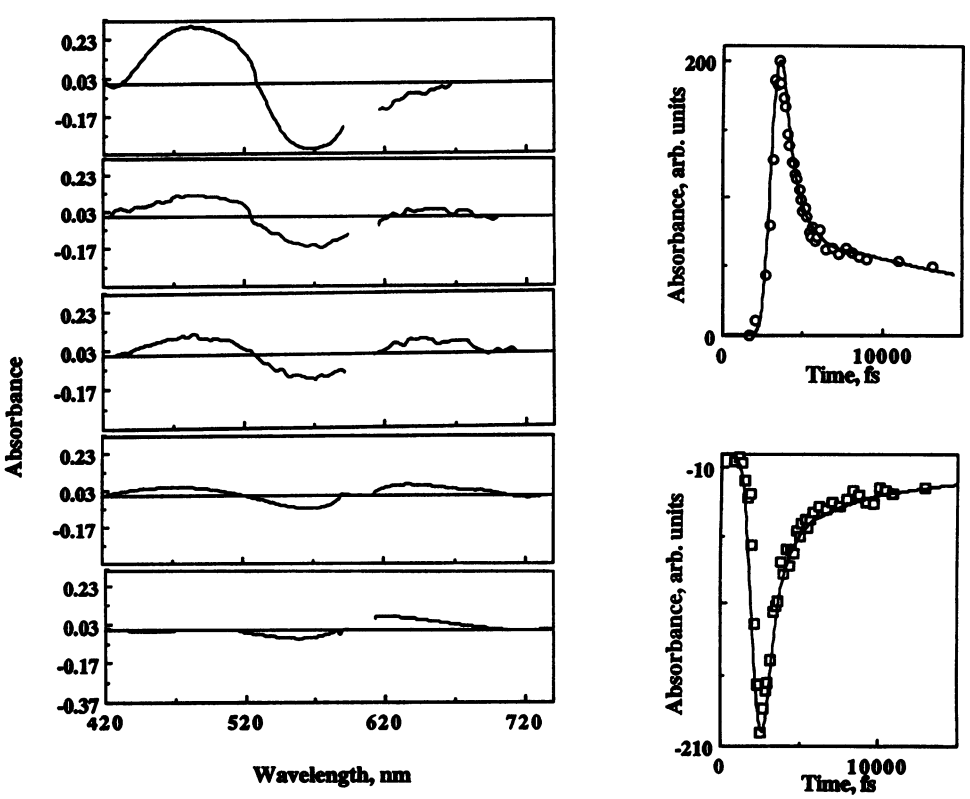

FIGURE 2 Transient absorption spectra, obtained after excitation by 500-fs laser pulse at 605 nm of W182F at the time delays of zero, 400 fs, 800 fs, 3.0 ps, and 40 ps. The inset at the top (○) shows kinetics at wavelength 470 nm and the best fit with parameters collected in Table 3 (*solid line*). The inset at the bottom (□) corresponds to the kinetics of the absorption changes at 570 nm and the best fit with parameters shown in Table 3 (*solid line*).

TABLE 3 The parameters of the best fit of the excited-state decay (wavelength 460–480 nm) and the recovery of the ground state (wavelength 560–580 nm) of the wild-type bR, and mutants W182F, A53G, and V49A

	Excited-state absorption				Ground-state bleaching				
	τ_1 (ps)	τ_2 (ps)	A	B	τ_3 (ps)	τ_4 (ps)	C	D	E
Wild-type	0.5 ± 0.1	5	0.95	0.05	0.5 ± 0.1	3	0.6	0.3	0.1
W182F	0.8 ± 0.1	20	0.8	0.2	0.8 ± 0.1	5	0.8	0.15	0.05
A53G	0.5 ± 0.1	5	0.82	0.18	0.5 ± 0.1	4	0.72	0.2	0.08
V49A	1.00 ± 0.08	20	0.82	0.18	0.90 ± 0.07	7	0.8	0.15	0.05

The best fit was obtained by the least-squares method after deconvolution of the measured kinetics with apparatus function of the subpicosecond spectrometer (*inset* at the bottom of Fig. 3) and multiexponential decay. The decay function was chosen as $(A\exp(-t/\tau_1) + B\exp(-t/\tau_2))$ for the excited-state decay and as $(C\exp(-t/\tau_3) + D\exp(-t/\tau_4) + E)$ for the ground-state recovery.

mate the limit of the quantum yield of photoisomerization of all-*trans* retinal for each mutant. The simple equation can be used:

$$\Phi_{ave} = \Phi_{all\text{-}trans}A + \Phi_{other}(1 - A), \quad (3)$$

where Φ_{ave} is an average (determined) quantum yield, A is the fraction of all-*trans* isomer, $\Phi_{all\text{-}trans}$ is the quantum yield of photoisomerization for the all-*trans* form of bR, and Φ_{other} is the quantum yield of photoisomerization for isomers different from the all-*trans* form. Assuming $\Phi_{other} = 1$, we obtain a lower limit value for $\Phi_{all\text{-}trans}$, and assuming $\Phi_{other} = 0$, we obtain a upper limit for $\Phi_{all\text{-}trans}$. The fraction of all-*trans* isomer, A, was taken as the contribution of the fast component in the excited-state decay kinetic (Table 3). The lower limits for $\Phi_{all\text{-}trans}$ using Eq. 3 were found to be 0.56 for W182F and 0.5 for V49A and A53G. The upper limits were found to be 0.8 for W182F and 0.75 for V49A and A53G. These values are only 15–20% different from Φ_{ave}, given in Table 2. This is not much different from the experimental error discussed previously. A similar approach can be applied to the estimation of lower and upper limits for the energy content of the K-intermediate, formed from the all-*trans* isomer. These values, again, are about 20% different from the average energy content determined for the mixture of different isomers in these mutants.

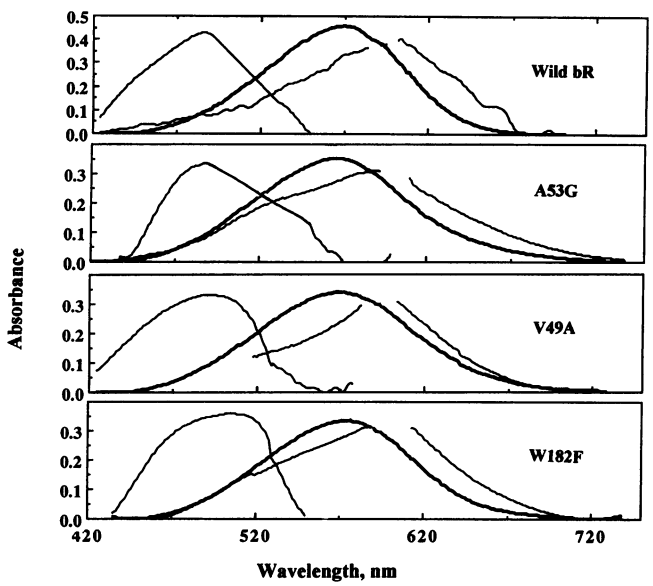

FIGURE 3 Spectra of the excited state, the ground state, and the K intermediate for wild-type bR (*A*), A53G, V49A, and W182F. The excited state spectra (on the left) were obtained by adding the ground-state spectra (*bold line*) to the transient spectra measured at time 0 (only the ground-state bleaching and the excited state are presented). The spectra for the K intermediate (on the right side) were obtained by adding the ground-state spectra (corrected for the quantum yield; see the text) to the transient, measured at the time of a few tens of picoseconds, where only the ground-state bleaching and the K intermediate are present. The ground-state spectra (*in the middle, bold line*) were obtained by subtraction of the background due to light scattering. The background was obtained by interpolation of sample absorption at wavelengths around 420 and 720 by second-order polynomial.

DISCUSSION

The lifetimes of the retinal excited states are found to be longer by a factor of 2 for V49A and by a factor of 1.7 for W172F when compared with wild-type bR. There is no change in the rate of isomerization of the A53G mutant. The quantum yields of isomerization of the studied mutants are not significantly changed. Using Eq. 1, and the quantum yield values from the previous section, it is possible to estimate the energy content of the K-intermediate. These numbers are shown in Table 2. We have to mention here the point made previously (Rohr et al., 1992a) that earlier cryogenic photocalorimetry measurements of the energy of the K-intermediate reported lower values than the room temperature photoacoustics (Birge et al., 1991) (about 50 kJ/mol). Photocalorimetry measures the energy storage in the fully equilibrated system between the chromophore, protein, and solvent, whereas the fast transient technique measures a nonequilibrated system. Comparison of the data for energy of the K-intermediate indicates that within the errors of our measurement there is no significant difference between the apparent quantum yields of these mutants and that of wild-type bR.

The average formation lifetime of the M intermediate is longer in V49A and W182F and shorter in A53G, in comparison to wild-type bR (Table 3). The fact that no changes are observed in the photoisomerization lifetime of A53G can suggest that such replacement does not lead to changes

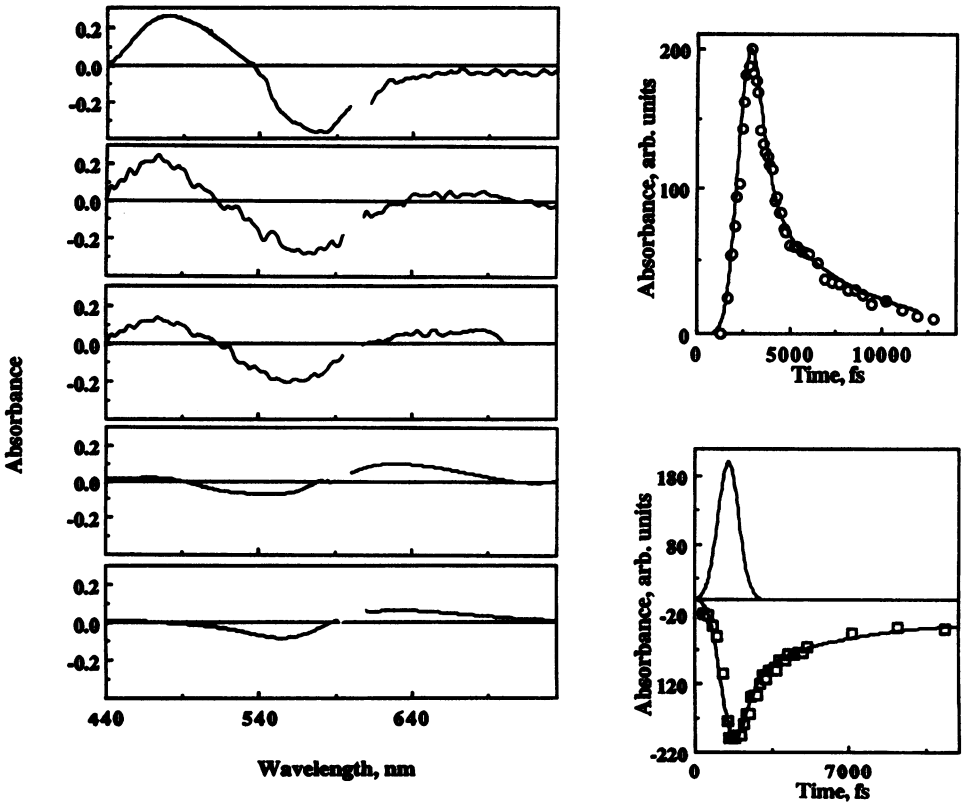

FIGURE 4 Transient absorption spectra, obtained after excitation by 500-fs laser pulse at 605 nm of A53G at the time delays of zero, 400 fs, 800 fs, 4.4 ps, and 7 ps. The inset at the top shows kinetics at wavelength 475 nm (○) and the best fit with parameters collected in Table 3 (*solid line*). The inset at the bottom corresponds to the kinetics of the absorption changes at 560 nm (□), the best fit with parameters shown in Table 3 (*solid line*), and the apparatus function (*positive signal*).

in the relevant charge distribution that controls the photoisomerization dynamics, or it brings the Schiff base and Asp85 in better orientation for proton transfer due to protein conformation changes occurring after the photoisomerization process. The changes in the rate of isomerization in W172F and V49A, however, affect neither the quan-

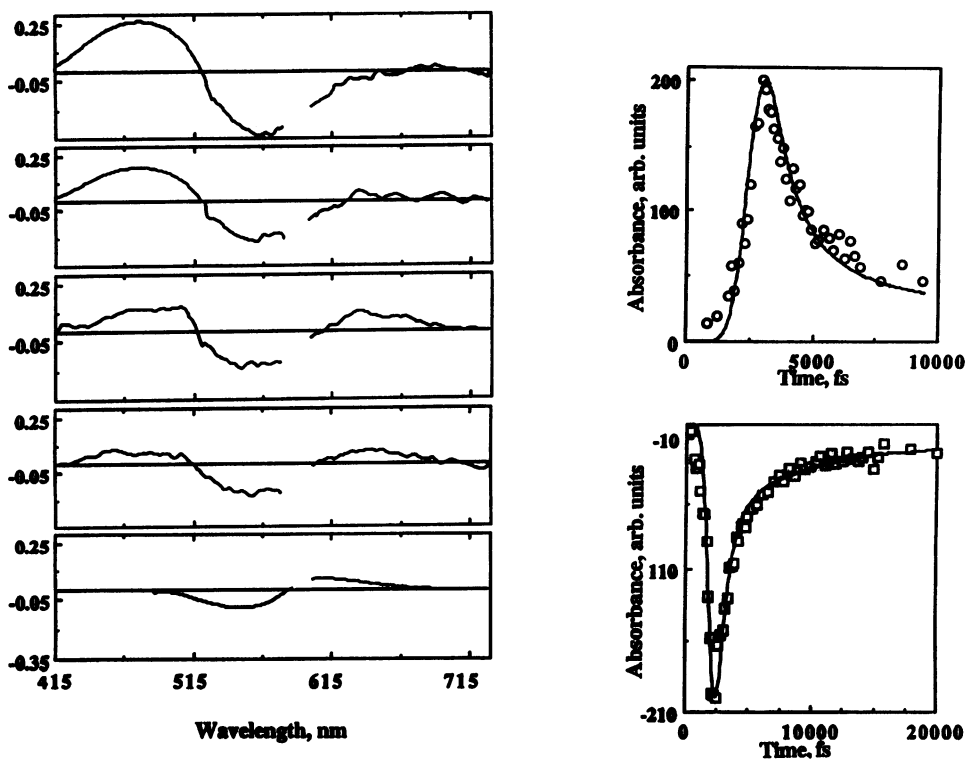

FIGURE 5 Transient absorption spectra, obtained after excitation by 500-fs laser pulse at 605 nm of V49A at the time delays of zero, 400 fs, 800 fs, 1.6 ps, and 40 ps. The inset at the top shows kinetics at wavelength 475 nm (○) and the best fit with parameters collected in Table 3 (*solid line*). The inset at the bottom corresponds to the kinetics of the absorption changes at 565 nm (□) and the best fit with parameters shown in Table 3 (*solid line*).

tum yield nor the energy content of the K-intermediate. These data and our previous measurements on the quantum yield and energy of the K-intermediate for other mutants (Logunov et al., 1996) show that there is no correlation between the rate of photoisomerization and the quantum yield of photoisomerization or the energy content of the K-intermediate. In cases when the rate of isomerization becomes slower than in wild-type bR, the quantum yield of photoisomerization and the energy content in the K-intermediate remain unchanged (assuming the light-adapted V49A and W182F mutants have an all-*trans* isomer), yet the other rates in the photocycles change significantly. This was explained previously (Logunov et al., 1996) by proposing an excited-state torsional potential that is flat and symmetric at a torsional angle of 90° (giving rise to insensitive isomerization yield), the separation of which from the top of the ground-state barrier (the energy gaps) changes with the retinal environment. Wild-type bR has the smallest gap and thus the shortest photoisomerization time. Changes in the charge distribution around the retinal from that present in the natural pigment can only increase the gap, either by decreasing the ground-state barrier to thermal isomerization or by raising the bottom of the excited-state surface at 90° (most likely the former). Because the rapid photoisomerization process in the natural pigment does not give rise to a corresponding larger photoisomerization yield or amount of energy stored, one concludes that the rapid photoisomerization assists in making the photoisomerization specific around the C_{13}-C_{14} bond. This can be understood as one realizes that photoisomerization around other bonds does not lead to proton transfer in the L $\rightarrow$ M process and thus does not lead to proton pumping. Thus nature was maximizing the proton pump yield by making the photoisomerization selective.

We thank the Department of Energy, Office of Basic Energy Sciences (grant DE-FG03-88ER-13828), for financial support.

REFERENCES

Birge, R. R., T. M. Cooper, A. F. Lawrence, M. B. Mosthay, C. F. Zhang, and R. J. Zidoretzki. 1991. Revised assignment of the energy storage in the primary photochemical event in bacteriorhodopsin. *J. Am. Chem. Soc.* 113:4327–4328.

Braiman, M. S., T. Mogi, L. J. Stern, H. G. Khorana, and K. Rothschild. 1988. Vibrational spectroscopy of bacteriorhodopsin mutants: light-driven proton transport involved protonation changes of aspratic acid residues 85, 96 and 212. *Biochemistry.* 27:8516–8520.

Braslavsky, S. E., and K. Heihoff. 1989. Photothermal methods. *In* Handbook of Organic Photochemistry, Vol. 1. J. C. Scaiano, editor. CRC Press, Boca Raton, FL. 327–356.

Brown, L. S., Y. Gat, M. Shelves, Y. Yamazaki, A. Maeda, R. Needleman, and J. K. Lanyi. 1995. The retinal Schiff base-counterion complex of bacteriorhodopsin: changed geometry during the photocycle is a cause of proton transfer to aspartate 85. *Biochemistry.* 11:12001–12011.

Goldschmidt, C. R., O. Kalinsky, T. Rosenfeld, and M. Ottolenghi. 1977. The quantum yield efficiency of the bacteriorhodopsin photocycle. *Biophys. J.* 17:179–183.

Henderson, R., J. M. Baldwin, T. A. Ceska, F. Zemin, E. Beckmann, and K. H. Downing. 1990. Model for structure of bacteriorhodopsin based on high resolution electron cryomicroscopy. *J. Mol. Biol.* 213:899–929.

Kobayashi, T., M. Terauchi, T. Kouyama, M. Yoshizawa, and M. Taiji. 1990. Femtosecond spectroscopy of acidified and neutral bacteriorhodopsin. *SPIE Laser Appl. Life Sci.* 1403:407–416.

Lanyi, J. K. 1993. Proton translocation mechanism and energetics of light-driven pump bacteriorhodopsin. *Biochim. Biophys. Acta.* 1183: 241–261.

Logunov, S. L., M. A. El-Sayed, L. Song, and J. K. Lanyi. 1996. Photoisomerization quantum yield and apparent energy content of the K-intermediate in the photocycles of bacteriorhodopsin, its mutants D85N, R82Q, D212N, and deionized blue bacteriorhodopsin. *J. Phys. Chem.* 100:2391–2398.

Logunov, S. L., L. Song, and M. A. El-Sayed. 1994. pH dependence of the rate and quantum yield of the retinal photoisomerization in bacteriorhodopsin. *J. Phys. Chem.* 98:10674–10677.

Mathies, R. A., C. H. Brito Cruz, W. T. Pollard, and C. V. Shank. 1988. Direct observation of the femtosecond excited-state cis-trans isomerization in bacteriorhodopsin. *Science.* 240:777–779.

Needleman, R., M. Chang, B. Ni, G. Varo, J. Fornes, S. H. White, and J. K. Lanyi. 1991. Properties of asp212-asp bacteriorhodopsin suggest that Asp212 and asp85 both participate in a counterion and proton acceptor complex near Schiff base. *J. Biol. Chem.* 266:11478–11484.

Oesterhelt, D., and W. Stoeckenius. 1974. Isolation of the cell membrane of *Halobacterium halobium* and its fractionation into red and purple membrane. *Methods Enzymol.* 31:667–678.

Petrich, J. W., J. Bretton, J. L. Martin, and A. Antonetti. 1987. Femtosecond absorption spectroscopy of light-adapted and dark-adapted bacteriorhodopsin. *Chem. Phys. Lett.* 137:369–375.

Rohr, M., W. Gartner, G. Schweitzer, and S. E. Braslavky. 1992a. Quantum yield of the photochromic equilibrium between bacteriorhodopsin and its bathointermediate K. Femto- and nanosecond optoacoustic spectroscopy. *J. Phys. Chem.* 96:6055–6061.

Rohr, M., G. Schweitzer, W. Gartner, and S. E. Braslavky. 1992b. Detection of conformational changes during the photocycle of bacteriorhodopsin by laser induced optoacoustic spectroscopy (LIOAS). *Struct. Funct. Retinal Proteins.* 221:151–154.

Schulenberg, P. J., M. Rohr, W. Gather, and S. E. Braslavsky. 1994. Photoinduced volume changes associated with the early transformations of bacteriorhodopsin: a laser-induced optoacoustic study. *Biophys. J.* 66:838–843.

Song, L., M. A. El-Sayed, and J. K. Lanyi. 1993. Protein catalysis of the retinal subpicosecond photoisomerization in the primary process of bacteriorhodopsin photosynthesis. *Science.* 261:891–894.

Song, L., D. Yang, M. A. El-Sayed, and J. K. Lanyi. 1995. Retinal isomer composition in some bacteriorhodopsin mutants under light and dark adaptation conditions. *J. Phys. Chem.* 99:10052–10055.

Tittor, J., and D. Oesterhelt. 1990. The quantum yield of bacteriorhodopsin. *FEBS Lett.* 263:269–273.

Wu, S., Y. Chang, M. A. El-Sayed, T. Marti, T. Mogi, and H. G. Khorana. 1992. Effect of tryptophan mutation on the deprotonation and reprotonation kinetics of the Schiff base during the photocycle of bacteriorhodopsin. *Biophys. J.* 61:1281–1287.

Xie, A. 1990. Quantum yield efficiencies of bacteriorhodopsin photochemical reactions. *Biophys. J.* 58:1127–1132.

Yamazaki, Y., J. Sasaki, M. Hatanaka, H. Kandori, A. Maeda, R. Needleman, T. Shinada, K. Yoshihara, L. S. Brown, and J. K. Lanyi. 1995. Interaction of tryptohan-182 with the retinal 9-methyl group in the L intermediate of bacteriorhodopsin. *Biochemistry.* 34:577–582.